Title: Analysis of Breast, Back and Butterfly Strokes by the Swimming Human Simulation Model SWUM

Short Title: Analysis of Breast, Back and Butterfly Strokes by SWUM

Author: Motomu Nakashima[1]

[1] Department of Mechanical and Environmental Informatics, Graduate School of Information Science and Engineering, Tokyo Institute of Technology, 2-12-1 Ookayama, Meguro-ku, Tokyo 152-8552, Japan

Key words: Swimming, Simulation, Fluid Force, Propulsive Efficiency, SWUM, Crawl, Breaststroke, Backstroke, Butterfly Stroke, Analysis, Stroke Length, Body Geometry, Joint Motion, Human, Limbs, Fluid Dynamics, Biomechanics, Normal Drag, Tangential Drag, Added Mass

Analysis of Breast, Back and Butterfly Strokes by the Swimming Human Simulation Model SWUM

Motomu Nakashima[1]

[1] Department of Mechanical and Environmental Informatics, Graduate School of Information Science and Engineering, Tokyo Institute of Technology, 2-12-1 Ookayama, Meguro-ku, Tokyo 152-8552, Japan

Summary. In the preceding study, the swimming human simulation model "SWUM" has been developed by the authors, and the analysis of standard six beat crawl stroke has been conducted. In this paper, the analyses of three strokes, that is, breast, back and butterfly strokes were conducted. The swimming motion, velocity in the propulsive direction of the human body, and the fluid force in the propulsive direction acting on the upper and lower limbs were respectively shown for those three strokes. In addition, the stroke length and the propulsive efficiency of the four strokes were investigated by the simulation. It was found that the stroke lengths of the crawl, back and butterfly strokes in the simulation agree significantly with the actual values, and that of the breaststroke becomes relatively smaller. It was also found that the propulsive efficiency of the crawl, back and butterfly strokes becomes around 0.2, although that of the breaststroke becomes only 0.036.

Key words. Swimming, Simulation, Fluid Force, Propulsive Efficiency, SWUM

1 Introduction

The authors have recently developed a simulation model for a self-propelled swimmer "SWUM" (SWimming hUman Model), which can represent the dynamics of the whole body and which has the potential to be a widely used tool for the analysis of various mechanical problems in human swimming (Nakashima et al. 2007). In this model, the fluid force is considered as simplified modeled force, and the equations of motion of the self-propelled swimmer's body in the translational and rotational directions are solved by the time integration. As inputs, the body geometry and relative body motion (joint motion) are given. As outputs, the swimming speed, rolling and yawing motions, joint torque and so on are obtained. An

analysis of the six beat crawl stroke has been already conducted, in which the joint motion data was input based on a video taken of an actual athlete swimming. It was found that the swimming speed obtained in the simulation agrees significantly with that of the video, indicating the validity of the simulation model. The authors have also investigated detailed characteristics of the six beat crawl, that is, the contribution of each fluid force component and each body part to the thrust, and computed the propulsive efficiency (Nakashima 2007). In this study, investigation similar to that conducted on the crawl stroke was performed on the other three strokes; those being: breast, back and butterfly strokes. In addition, comparison among the four strokes was made from the viewpoint of mechanics.

2 Analysis Method

2.1 Overview of SWUM

In SWUM, the relative body motion as the joint angles is given for the human body, which is modeled as rigid link segments. The absolute motion of the whole body is computed considering the unsteady fluid force acting on the human body. The human body is represented by a series of 21 truncated elliptical cone segments. With respect to the fluid force, the inertial force due to the added mass of the fluid, the drag force in the normal and tangential directions, and buoyancy are taken into account. In order to compute the inertial force due to the added mass and the drag forces in the normal and tangential directions, fluid force coefficients are invoked. These coefficients have been determined by an experiment in which a model of a human limb was flapped in the water, measuring its motion and fluid force. The details are described in the previous paper (Nakashima et al. 2007).

2.2 Analysis Condition

The joint motions as input data for the simulation model were determined based on videos of ‘model swimming’ (IPA 2004), which were produced by the Japan Swimming Federation and open to the public for educational purposes. Note that the swimming motions in the videos are not full strength competitive ones because of their educational purposes. One cycle of the swimming motion was divided into 18 frames. The joint angles at each frame were manually determined so that the body position in the video at the corresponding frame becomes as close to that in the simulation

as possible. The given number of degrees-of-freedom of the joint rotations for breast stroke was 34 ; for back, 28 ; and for butterfly, 35.

All the quantities in the simulation were computed in a system normalized by time, length, and density. Their reference values are, respectively, stroke cycle, swimmer's stature, and the water density. The body geometry was set as that of an average 20-29 year-old Japanese male. The body height and weight are 1.705 m and 64.9 kg, respectively. The hydrostatic lift, which is defined as the difference between the net buoyancy and body weight, is 22.5 N (2.3 kgf). According to Chatard et al. (1990), the hydrostatic lift for swimmers are 17~29 N (1.7~3.0 kgf). The value of 22.5 N in the present model is almost at the center of that range. The number of divisions of each truncated elliptical cones for longitudinal and circumferential directions were, respectively, 10 and 36. The time step was set as 0.002, that is, 500 steps for one stroke cycle.

3 Results and Discussion

3.1 Breaststroke

Figure 1 shows the simulation results of the swimming motion for one cycle after nine stroke cycles, that is, after the effect of initial condition disappears. The water surface is colored with dark and pale colors alternatively. The area width of one color represents half of the stroke length. Therefore, the total width of one set of dark and pale areas corresponds to the stroke length. The dark sticks from each of the swimmer's body parts represent the direction and magnitude of the fluid force, except buoyancy. Figure 2 shows the velocity of the center of mass for the swimmer's body in the propulsive direction. Figure 3 shows the fluid force acting on the right upper and lower limbs in the same direction. Note that the negative value in these graphs corresponds to the positive propulsive speed and thrust. From these figures, it is found that the swimmer's body first accelerates due to the thrust generated by the hand at t = 9.3, and accelerates again significantly due to the large thrust generated by the kick of the legs. For the breaststroke, it is generally known that the propulsive velocity has two positive major peaks due to the upper and lower limbs. The peak value due to the lower limb (kick) is known to be almost equal to or slightly greater than that due to the upper limb (hand stroke) (Maglischo 2003). However, the peak due to the lower limb in the simulation at t = 9.7 is smaller than that due to the upper limb at t = 9.4. One possible reason for this inconsistency may be that the thrust generated by the kick is underestimated in the simulation due to the modeling error for the fluid force.

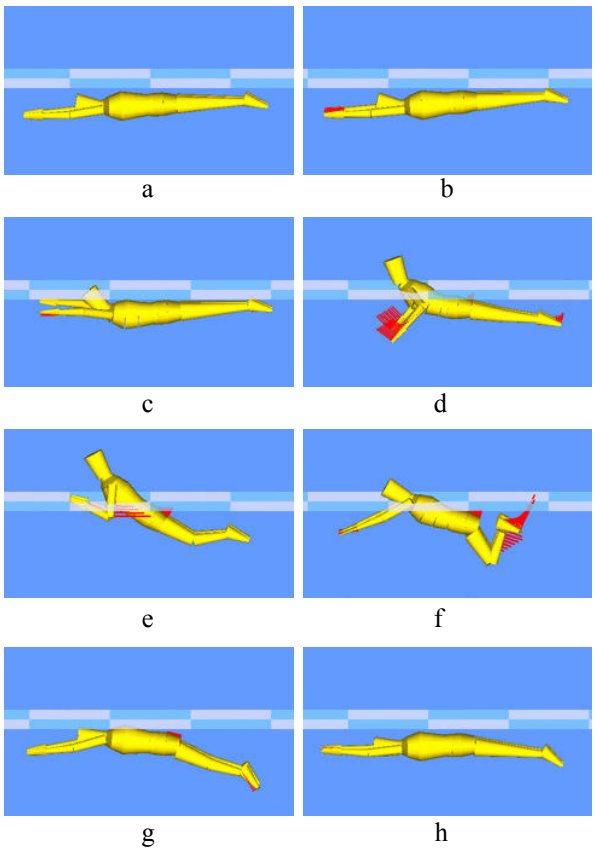

Fig. 1. Simulation results of swimming motion for one cycle from the side view (Breaststroke). a: $t = 9.0$. b: $t = 9.125$. c: $t = 9.25$. d: $t = 9.375$. e: $t = 9.5$. f: $t = 9.625$. g: $t = 9.75$. h: $t = 9.875$.

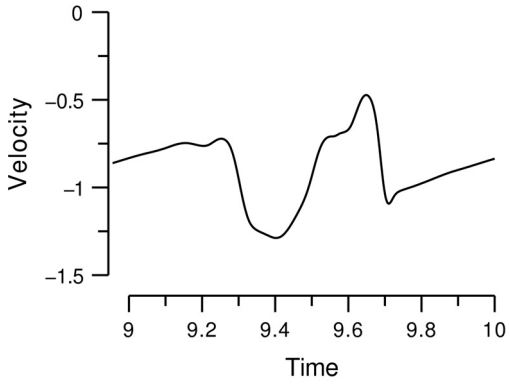

Fig. 2. Velocity of center of mass in propulsive direction (Breaststroke).

With respect to the fluid force components to the thrust, it is found that the thrust of the upper limb is mainly generated by the normal drag force, and the thrust of the lower limb is generated by the inertial force due to the added mass of the fluid as well as the normal drag force. It is also found that both the upper and lower limbs produce negative thrust at $t = 9.5$ and 9.6, respectively, that is, at the recovery motions for them. In particular, the negative thrust by the upper limbs around $t = 9.5$ seems to be unnaturally large. This causes deceleration during $t = 9.4$~9.6, resulting the reduction of the averaged swimming speed.

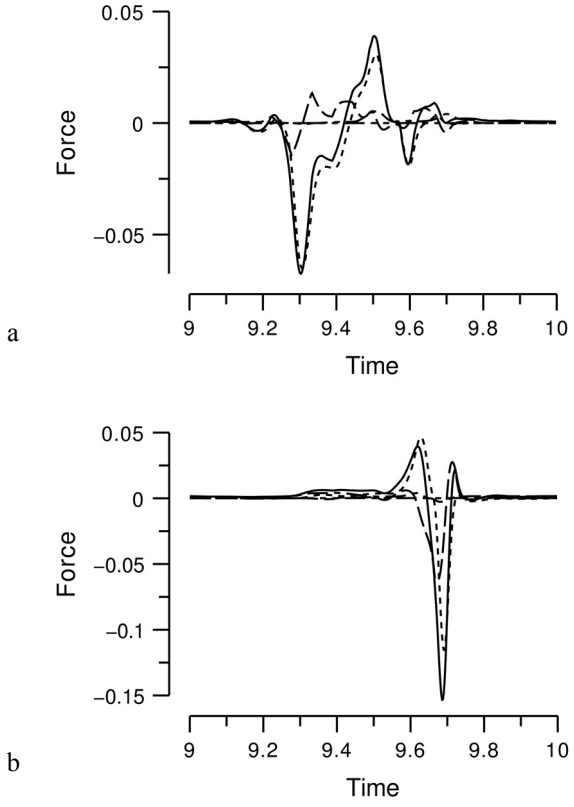

Fig. 3. Fluid force acting on right limbs in propulsive direction (Breaststroke). a: upper limb. b: lower limb. Solid line: total of all components. Long-dashed line: inertial force due to added mass. Short-dashed line: normal drag. Dot-dashed line: tangential drag. Two-dot-dashed line: buoyancy.

3.2 Backstroke

Figure 4 shows the simulation results of the swimming motion for a half cycle. Figure 5 shows the velocity of the center of mass for the swimmer's body in the propulsive direction. Figure 6 shows the fluid force acting on the right upper and lower limbs in the same direction. It is found that the thrust by the hand is large, the same as in the crawl stroke (Nakashima 2007), and it reaches its maximum, due to the normal drag force, at $t = 9.3$, that is, at the hand's 'push' motion. Immediately following, the velocity reaches its maximum. With respect to thrust of the lower limb, three major negative peaks appear in the flutter kick, and the primary components of them are found to be the inertial force due to the added mass and the normal drag.

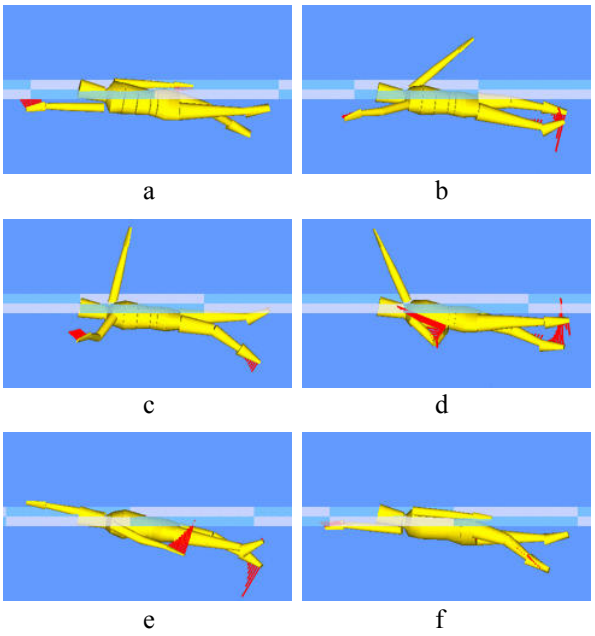

Fig. 4. Simulation results of swimming motion for a half cycle from the side view (Backstroke). a: $t = 9.0$. b: $t = 9.1$. c: $t = 9.2$. d: $t = 9.3$. e: $t = 9.4$. f: $t = 9.5$.

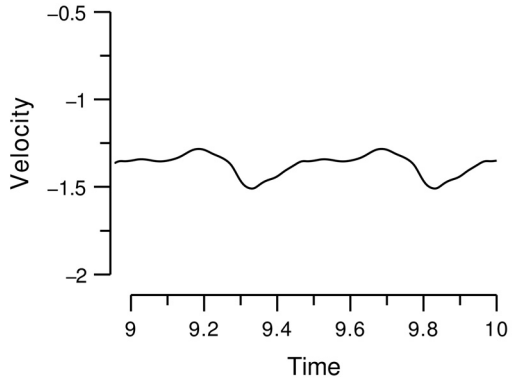

Fig. 5. Velocity of center of mass in propulsive direction (Backstroke).

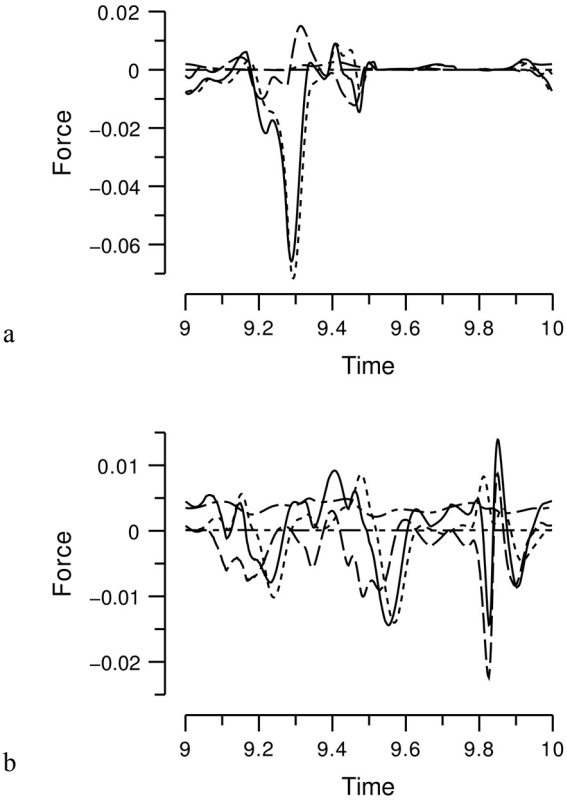

Fig. 6. Fluid force acting on right limbs in propulsive direction (Backstroke). a: upper limb. b: lower limb. Solid line: total of all components. Long-dashed line: inertial force due to added mass. Short-dashed line: normal drag. Dot-dashed line: tangential drag. Two-dot-dashed line: buoyancy.

3.3 Butterfly Stroke

Figure 7 shows the simulation results of the swimming motion for one cycle. Figure 8 shows the velocity of the center of mass for the swimmer's body in the propulsive direction. Figure 9 shows the fluid force acting on the right lower and upper limbs in the same direction. With respect to the upper limb, it is found that the large thrust is generated by the hand's motion, which starts from $t = 9.2$, reaches its peak at $t = 9.55$; with the velocity reaching its peak concomitantly. With respect to the lower limb, it is found that the thrust is generated by the weaker kick at $t = 9.45$, and by the stronger one at $t = 9.9$. It is also found that almost all the thrust by the upper limb is due to the normal drag force, and the thrust by the lower limb is generated by the inertial force due to added mass and the normal drag force.

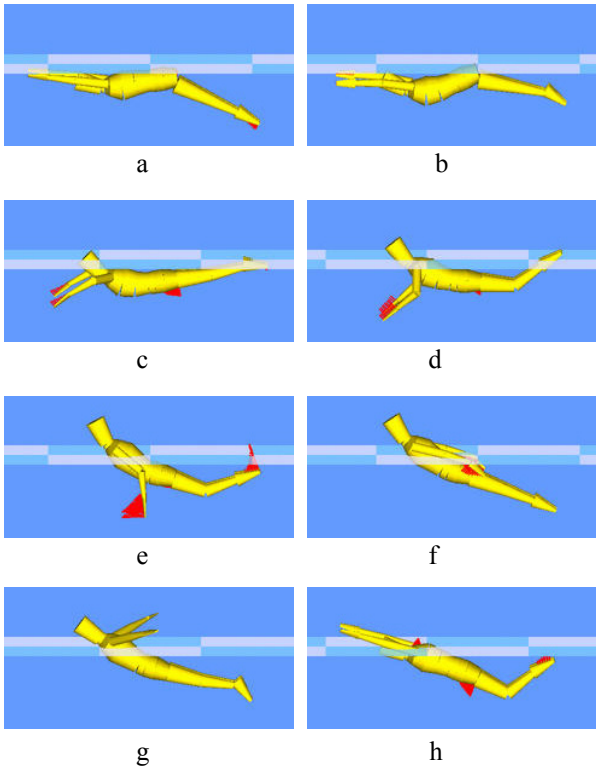

Fig. 7. Simulation results of swimming motion for one cycle from the side view (Butterfly stroke). a: $t = 9.0$. b: $t = 9.125$. c: $t = 9.25$. d: $t = 9.375$. e: $t = 9.5$. f: $t = 9.625$. g: $t = 9.75$. h: $t = 9.875$.

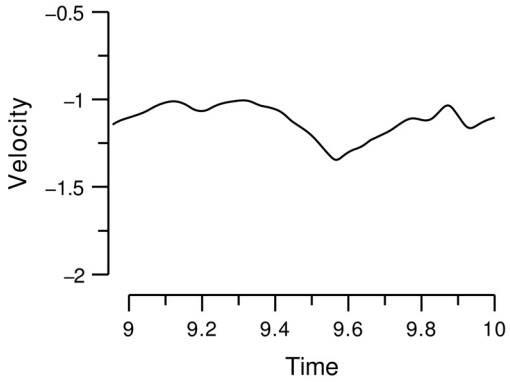

Fig. 8. Velocity in propulsive direction (Butterfly stroke).

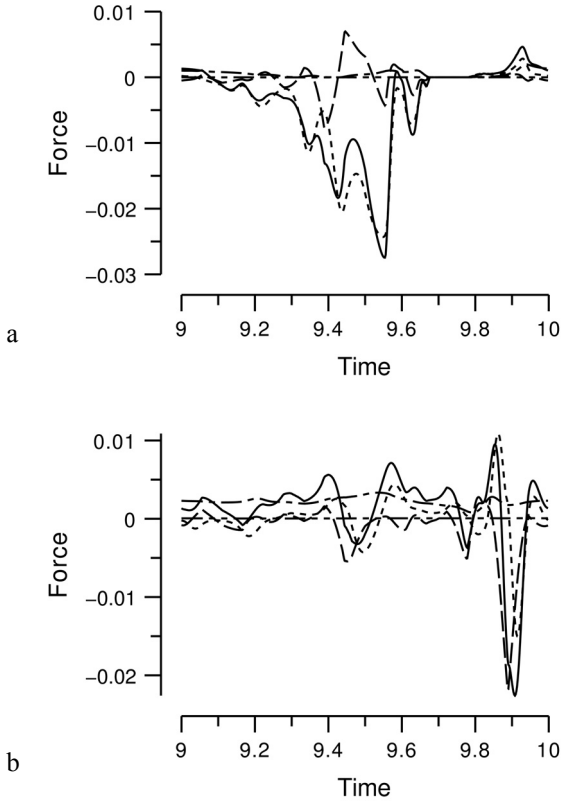

Fig. 9. Fluid force acting on right limbs in propulsive direction (Butterfly stroke). a: upper limb. b: lower limb. Solid line: total of all components. Long-dashed line: inertial force due to added mass. Short-dashed line: normal drag. Dot-dashed line: tangential drag. Two-dot-dashed line: buoyancy.

3.4 Comparison Among Four Strokes

Based on the analyses in the previous sections, the comparison between the four strokes including the crawl is made in this section. Figure 10 shows the results of comparison for the normalized stroke length, which represents the distance traveled in one stroke cycle divided by the swimmer's stature. The actual values of the normalized stroke length, which were estimated from the video, are also shown in the figure. The simulation results are found to agree significantly with the actual values for the three strokes of the crawl, back, and butterfly strokes. This agreement indicates the validity of the simulation model. However, the simulation result for the breaststroke is considerably smaller (about 35%) than the actual value. Two possible reasons for this discrepancy are that the thrust due to the kick is underestimated, and that the drag of the upper limbs in the recovery motion reduces the stroke length, as stated in section 3.1.

Next, Fig. 11 shows the analysis results of the propulsive efficiency; which is defined by:

$$\eta = \frac{UT}{P} \tag{1}$$

where U, T, and P respectively represent the swimming speed averaged in one cycle, the drag acting on the swimmer's body towed at the speed U with the gliding position, and the averaged mechanical power consumed by the swimmer. From the figure, it is found that the values of η are about 0.2 for the crawl, back, and butterfly strokes, whereas it is considerably smaller (about 0.036) for the breaststroke. Even if it is acknowledged that the stroke length in the simulation becomes smaller as shown in Fig. 10, it can still be said that the breaststroke is less efficient than the other three strokes.

Note that the propulsive efficiency defined in this study corresponds to

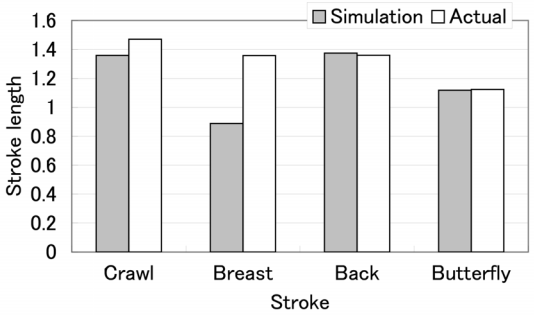

Fig. 10. Results of normalized stroke length for four strokes.

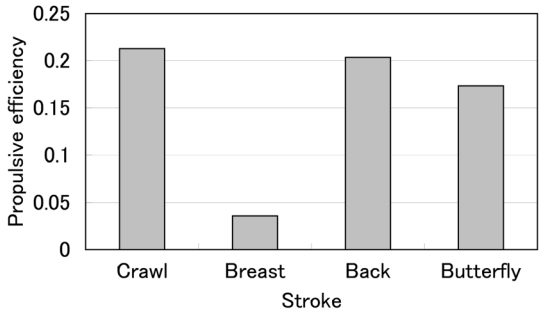

Fig. 11. Results of propulsive efficiency for four strokes.

the 'propelling efficiency' in Toussaint et al. (1988), and they reported its value to be 0.46~0.77 for the crawl due to their subjective experiment. The simulation results in this study are considerably smaller than those. It is possible that the present simulation underestimates the propulsive efficiency by some reasons. However, it may be also possible that the previous results of 0.46~0.77 overestimate it. For example, the propulsive efficiency of a high-performance-type screw propeller is generally known to be about 0.7. The propulsive efficiency of a dolphin robot, which has been developed by the authors, and has a streamlined body and a wing-shaped caudal fin, was also found to be 0.7 in the best condition (Nakashima and Ono 2002). It is hard to believe that the propulsive efficiency of the human swimming may exceed those of the screw propeller and the dolphin-type swimming since human has neither the screw propeller, nor the streamlined body, nor the wing-shaped fin. Further investigation is undoubtedly necessary in order to conclude this discussion.

4 Conclusions

In this paper, the breast, back, and butterfly strokes were analyzed using the swimming human simulation model SWUM. In addition, a comparison was made among the four strokes including the crawl from the viewpoint of mechanics. Findings are summarized as follows:

1. In the simulation of the breaststroke, the thrust due to the kick tends to be underestimated and the negative thrust by the upper lilmbs tends to be overestimated. Therefore, the swimming speed in the simulation becomes 35% less than the actual value.
2. The swimming speeds of the crawl, back, and butterfly strokes agree significantly with the actual values, indicating the validity of the

simulation model.

3. As a result of the comparison among the four strokes, it is found that the propulsive efficiency is about 0.2 for the crawl, back, and butterfly strokes, whereas it is considerably smaller (about 0.036) for the breaststroke.

All information about SWUM and its implementation software Swumsuit, as well as the animation of the simulation results which are shown in this paper, are open to the public at the website (http://www.swum.org/).

References

Chatard JC, Lavoie JM, Lacour JR (1990) Analysis of determinants of swimming economy in front crawl. Eur. J. of Appl. Physiology, 61:88-92

IPA (Information-technology Promotion Agency, Japan) (2004)
http://www2.edu.ipa.go.jp/gz/h1swim/ (in Japanese)
(Videos of each stroke are located as below:
Crawl: http://www2.edu.ipa.go.jp/gz/h1swim/h1kn20/h1cr10/h1cr11.mpg,
Breast: http://www2.edu.ipa.go.jp/gz/h1swim/h1br00/h1br10/h1br11.mpg,
Back: http://www2.edu.ipa.go.jp/gz/h1swim/h1ba00/h1ba10/h1ba11.mpg,
Butterfly: http://www2.edu.ipa.go.jp/gz/h1swim/h1bu00/h1bu10
/h1bu11.mpg)

Maglischo EW (2003) Swimming fastest. Human Kinetics, pp 228-231

Nakashima M (2007) Mechanical study of standard six beat front crawl swimming by using swimming human simulation model. J. Fluid Science and Technology, (in press)

Nakashima M, Ono K (2002) Development of a two-Joint dolphin robot. In: Ayers J, Davis JL, Rudolph A (Eds) Neurotechnology for biomimetic robots, MIT Press, Cambridge Massachusetts, pp 309-324

Nakashima M, Miura Y, Satou K (2007) Development of swimming human simulation model considering rigid body dynamics and unsteady fluid force for whole body. J. Fluid Science and Technology, 2(1):56-67

Toussaint HM, Beelen A, Rodenburg A et al. (1988) Propelling efficiency of front-crawl swimming. J. Appl. Physiol. 65:2506-2512